In Vivo Brillouin Analysis of Lens Nucleus and Cortex in Adult Myopic Eyes and Their Correlation With Accommodation

Le Chang,[1] Fen Song,[1] Shijia Qu,[1] Huazheng Cao,[2] Yanan Wu,[3] Lulu Xu,[3] Jing Wang,[1] Ruirui Zhang,[1] Chao Xue,[3] and Yan Wang[3,4]

[1]Clinical College of Ophthalmology, Tianjin Medical University, Heping District, Tianjin, China
[2]School of Medicine, Nankai University, Nankai District, Tianjin, China
[3]Tianjin Eye Hospital, Tianjin Key Laboratory of Ophthalmology and Visual Science, Tianjin Eye Institute, Nankai University Affiliated Eye Hospital, Heping District, Tianjin, China
[4]Nankai University Eye Institute, Nankai University, Nankai District, Tianjin, China

Correspondence: Yan Wang, Tianjin Key Laboratory of Ophthalmology and Visual Science, Tianjin Eye Hospital, Tianjin Eye Institute, Nankai University Affiliated Eye Hospital, No. 4, Gansu Rd., Heping District, Tianjin 300020, China; wangyan7143@vip.sina.com.

LC and FS contributed equally to this study.

Received: November 13, 2024
Accepted: March 6, 2025
Published: April 2, 2025

Citation: Chang L, Song F, Qu S, et al. In vivo Brillouin analysis of lens nucleus and cortex in adult myopic eyes and their correlation with accommodation. *Invest Ophthalmol Vis Sci.* 2025;66(4):6. https://doi.org/10.1167/iovs.66.4.6

Purpose. The purpose of this study was to investigate the in vivo biomechanical properties of crystalline lens nucleus and cortex in adults with myopia, their potential influences, and the correlation between these properties and ocular accommodation.

Methods. The study included 195 right eyes of 195 participants, divided into 4 groups based on spherical equivalent: emmetropia (37 eyes), low myopia (41 eyes), moderate myopia (59 eyes), and high myopia (58 eyes). Participants underwent comprehensive ophthalmological examinations, including intraocular pressure, axial length, cycloplegic refraction, lens morphology, accommodation measurements, and Brillouin optical scanning of the lens. Additionally, demographic information, such as age and sex, was recorded. Normality tests were performed on the data using the Kolmogorov–Smirnov test. Between-group differences were examined using the Kruskal-Wallis test. Correlation and multiple regression analyses were conducted to analyze the factors associated with lens biomechanical properties and accommodation.

Results. The mean longitudinal modulus of the crystalline lens nucleus (LMN), anterior cortex (LMAC), and posterior cortex (LMPC) was 3.395 ± 0.027 GPa, 3.030 ± 0.066 GPa, and 2.990 ± 0.066 GPa, respectively, in adult myopia and 3.342 ± 0.024 GPa, 3.015 ± 0.0488 GPa, and 2.978 ± 0.049 GPa, respectively, in emmetropia. LMN was significantly higher in myopia (difference = 0.047, 95% confidence interval [CI] = 0.037 to 0.057, $P < 0.001$) and increased significantly with higher degrees of myopia (standardized $\beta = -0.712$, $P < 0.001$). No statistical differences in the LMAC or LMPC were observed between myopia and emmetropia. Lens densitometry on the centerline was the only lens parameter independently correlated with LMN (standardized $\beta = -0.282$, $P < 0.01$). Increased LMN in myopia was independently correlated with increased amplitude of accommodation (AMP) and decreased accommodative facility (AF; standardized $\beta = 0.198, -0.237$, all $P < 0.05$).

Conclusions. LMN was significantly higher in adult patients with myopia than in emmetropia and increased with increasing myopia. Increased LMN in myopia significantly correlated with decreased AF and increased AMP. High LMN may be an important biological alteration during the development of adult myopia, especially high myopia, providing new insights into myopia pathogenesis.

Keywords: myopia, crystalline lens, morphology, accommodation, biomechanic, Brillouin microscopy

Myopia is the leading cause of distance vision impairment globally.[1] Higher degrees of myopia can cause further irreversible visual damage through complications, such as myopic macular degeneration, cataracts, retinal detachment, and glaucoma.[1–3] With increasing global myopia, investigating its pathogenesis is key to prevent and control its spread. The crystalline lens, an essential part of the eye's refractive system, changes shape mainly through accommodation to meet changing visual needs, and its morphological and functional alterations play important roles in myopia formation.[4–8] Lens biomechanical properties are key to the maintenance of lens morphology and its response to accommodation demands.[9–11] Although more and more researchers have begun to focus on lens alterations in myopia, traditional studies have focused only on the indicators such as axial length (AL), lens curvature, and lens

refractive power,[5,7,8,12] with few in-depth studies on lens biomechanical properties in myopia. The in vivo biomechanical properties of the lenses in myopia and their correlation with accommodation are unknown, which limits our understanding of the pathogenesis of this condition.

Because of its position inside the eye, in vivo detection of the lens is challenging. Most previous investigations on lens biomechanics, such as lens spinning, indentation, and bubble acoustic, have been conducted in an in vitro environment.[13–17] The resulting lens mechanical data from these measurement techniques are highly variable and do not represent the mechanical properties of in vivo lenses.[13,16,18–20] This study introduces the Brillouin Optical Scanning System (BOSS), a novel optical imaging technique for detecting in vivo biomechanical properties of lenses.[18,21] This technology utilizes the Brillouin light-scattering principle to provide non-contact measurements of tissue mechanical properties with 3D cellular level resolution of tissue mechanical spatial variability maps by detecting the direct relationship between the spectral shift of the laser beam as it is scattered from the local tissue and the longitudinal elastic modulus of the tissue.[18,22–25] The Brillouin microscopy (BLS) was used to characterize changes in longitudinal modulus of the lens with age, and it was found that expansion of the central stiffening region of the lens may be a major contributing factor to age-related lens stiffening, with spatial distribution maps showing a gradient from the softer cortex to the stiffer nucleus.[18,26,27] These studies demonstrate the unique ability of BLS to assess in vivo ocular tissue mechanics but focus mainly on age-related changes, without addressing the relationship between lens biomechanics and myopia or their role in accommodation. Therefore, this study examines the lens biomechanics in patients with myopia and their link to accommodative function, extending BLS applications to a new clinical context.

Therefore, this cross-sectional study proposed the use of the BOSS aiming to investigate the in vivo biomechanical properties of lenses in myopia and analyze the potential factors affecting the lens biomechanical properties in conjunction with clinical indicators, such as age, sex, spherical equivalent (SE), lens morphology parameters, and AL. Additionally, we investigated the association between lens biomechanical properties and ocular accommodation, such as the amplitude of accommodation (AMP) and accommodative facility (AF), to provide new insights into the pathogenesis of myopia.

Methods

Participants

This cross-sectional study was conducted at the Refractive Surgery Center in Tianjin Eye Hospital, Clinical College of Ophthalmology, Tianjin Medical University. The study protocol was approved by the Ethical Review Committee of Tianjin Eye Hospital (No. KY-2024003). The study procedures followed the principles of the Declaration of Helsinki, and written informed consent was obtained from all participants before enrollment.

This study recruited 195 adult patients attending the outpatient clinic of the Refractive Surgery Center of Tianjin Eye Hospital from November 2023 to May 2024, and only the right eye was included. Inclusion criteria included: (1) best-corrected visual acuity (decimal visual acuity) $\geq$1.0; (2) clear refractive media; and (3) normal pupillary reflex to light. The exclusion criteria were as follows: (1) history of ocular disease, including keratoconus, glaucoma, cataract, or vitreoretinal disease; (2) organic ocular disease other than myopia complicating the eye; (3) history of ophthalmological surgery or ocular trauma; and (4) use of soft contact lenses within the last 2 weeks or orthokeratology lenses within the last 4 weeks. For analysis, the eyes were divided into four groups according to their SE values[28,29]: (A) emmetropia (0.5 diopter [D] > SE > −0.5 D), (B) low myopia (−0.5 D $\geq$ SE > −3 D), (C) moderate myopia (−3 D $\geq$ SE > −6 D), and (D) high myopia (SE $\leq$ −6 D).

Routine Examinations

All participants underwent a series of ocular examinations, including visual acuity (uncorrected distance and best-corrected distance), slit-lamp examination, and funduscopic examination. Intraocular pressure (IOP) was measured using a non-contact tonometer (Cannon Inc., Japan), and the average value was recorded after three measurements. AL was measured using IOLMaster 900 (Haag-Streit AG, Switzerland), and the test was repeated if the difference between 2 consecutive AL readings was >0.02 mm. Biometric parameters of the lenses under refractive status correction of the participants, including lens thickness (LT), lens diameter (LD), radius of curvature of the anterior and posterior surfaces of the lens, and lens optical density, were obtained using CASIA2 (TOMEY, Japan). Ocular accommodation, including AMP and AF, was tested after correcting for the subject's refractive state. AMP was detected in participants using the minus lens method. Subjects fixated on a near target at 40 cm while wearing their best-corrected distance prescription. Minus lenses were introduced in 0.25 D increments until sustained blur was reported, and the AMP was calculated as the sum of the total minus lens power added and the accommodative demand of the target (2.5 D). AF was measured using flippers: a 20/30-sized optotype was placed 40 cm in front of the participant's eyes, and a ±2.00 D handheld flipper was alternately placed in front of the participant's eyes, and the number of cycles in which the participant could see the optotype clearly was recorded for 1 minute. The accommodation parameters included in this study were monocular data, excluding the interference from binocular fusion factors. The patients underwent subjective optometry by professional optometrists to confirm their refractive status. All examinations were performed from 10 AM to 3 PM daily to minimize the influence of the circadian rhythm.

Brillouin Microscopy Examination

The BOSS (Intelon Optics, Boston, MA, USA) is classified as an ANSI Z80.36 group 1 instrument for all single and combined light sources used in the instrument. The beam from the laser source of the BOSS is collimated to a diameter of 3.3 mm, undergoes divergence and convergence along the beam path, and is ultimately focused on the lens (with a focused beam diameter of approximately 5 µm). The light scattering produced by the Brillouin effect is imaged by BOSS and analyzed using an integrated high-resolution spectrometer to determine the spectral offset of the laser beam (Fig. 1A). Longitudinal modulus of elasticity was calculated using the wavelength shift determined by the spectrometer based on established scientific relationships. Brillouin longitudinal modulus (M) was calculated from the

Investigative Ophthalmology & Visual Science

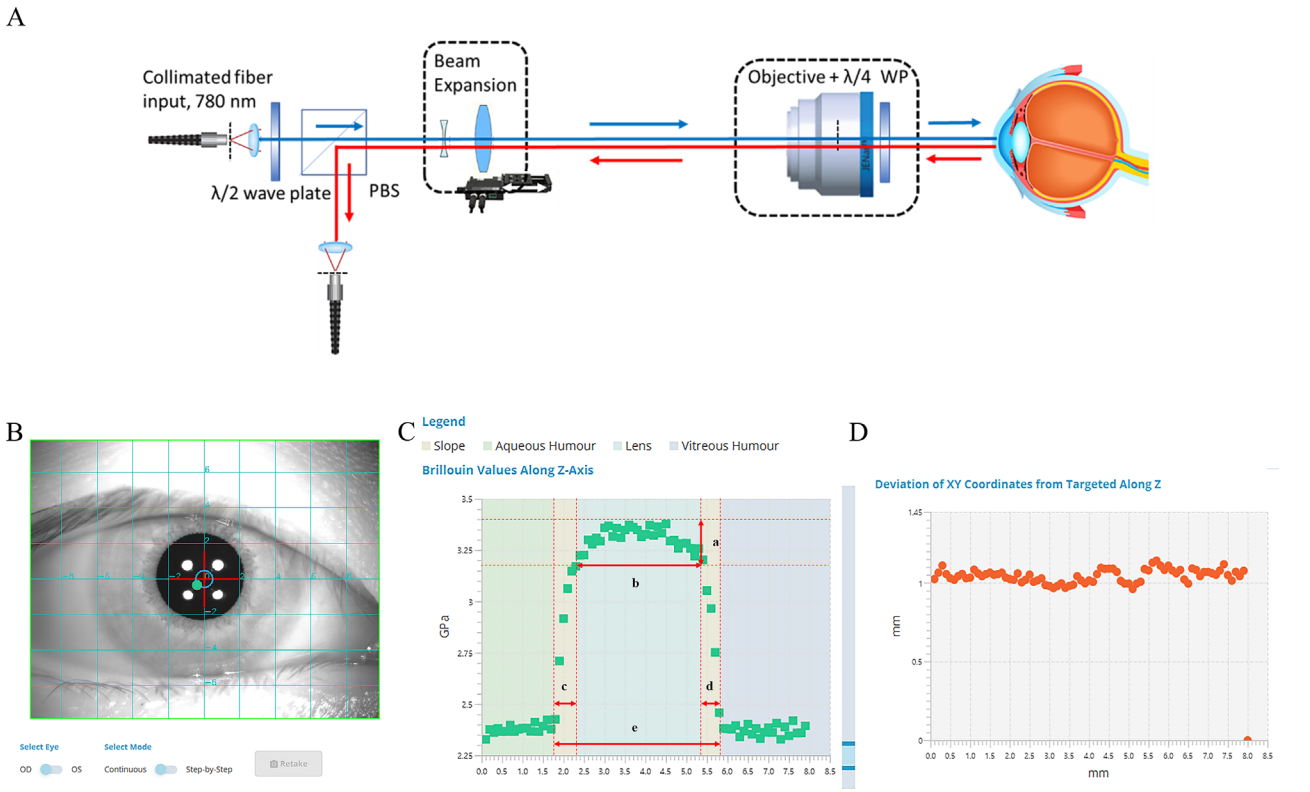

Figure 1. Schematic diagram of the Brillouin optical scanning system. (**A**) Schematic diagram of the optical path of the Brillouin optical scanning instrument (BOSS; Intelon Optics, Boston, MA, USA). (**B**) Software page for imaging acquisition of the participant's lens using the BOSS (Intelon Optics, Boston, MA, USA) in "Lens 1 pt" mode. (**C**) Axial profile map of the lens presented after optical scanning of Brillouin. (**A**) Longitudinal modulus of nucleus (LMN), the LMN is defined as the value of the average longitudinal modulus of the width of top plateau region. (**B**) Width of top plateau (WTP) represents the thickness of the lens nucleus and is defined as the region with the top 50% values of the Brillouin modulus. (**C**) Represents the anterior cortical region of the lens, (**D**) represents the posterior cortical region of the lens. (**E**) Width of bottom plateau (WBP) represents the thickness of the lens and is defined as the region with the top 98% values of the Brillouin modulus. (**D**) Plot of fluctuations in ocular pupil position during optical scanning of the lens by Brillouin.

Brillouin frequency shift (υB) according to the following relationship[18,21–25]:

$$M = \frac{\rho \upsilon B^2 \lambda^2}{4n^2 sin^2\left(\theta/2\right)}$$

where ρ is the mass density, λ (780 nm) is the optical wavelength in air, n the refractive index, and θ is the angle between incident and scattered light (180 degrees in our experimental condition). The ratio of ρ/n^2 was treated as a constant value of 0.5636 g/cm^3, consistent with the approach used by Besner et al.[18] for human lenses. The Brillouin frequency shift (υB) can be expressed as:

$$\upsilon B = \frac{2n}{\lambda} V \cos\left(\frac{\theta}{2}\right)$$

where V is the acoustic velocity. The laser power used in this experiment was 5 mW, which complies with the safety guidelines established by the International Commission on Non-Ionizing Radiation Protection (ICNIRP) for lens and cornea thermal hazards.[30] The same experienced physician examined the patient's lenses using BOSS's "Lens 1 pt" mode, ensuring that the measurement point was as close as possible to the center of the pupil, with no more than 1 mm deviation from the center of the pupil, in order to obtain data on the patient's lenses (Figs. 1B, 1C). The theoretical basis of this device for the detection of ocular longitudinal modulus and the delineation of the region of longitudinal modulus of the lens is derived from the study of Besner et al.[18] All participants were examined in a dark room at a temperature of 22 to 24°C. Participants were instructed to gaze at a fixed point generated by an LED light source, which was optically set at infinity to ensure relaxed accommodation during the measurement. Participants were asked to try to avoid intentional rapid blinking or excessive movement during the measurement, and the scanning process lasted approximately 50 seconds. Natural blinking was allowed throughout the test to maintain tear film stability and ocular comfort. Patient lenses were examined multiple times, and the average of the three scans with a Weighted Quality of "GOOD" and little fluctuation in pupil position was included in the subsequent statistical analyses. As shown in Figure 1D, "little fluctuation" refers to a trajectory that approximates a horizontal line, indicating stable pupil positioning throughout the measurement. Scans with significant deviations or irregular patterns were excluded from the analysis.

Statistical Analysis

Sample sizes were calculated using PASS (version 15.0; NCSS Statistical Software, Kaysville, UT, USA) based on the

results of the pretest, and a sample size of >26 patients in the different refractive groups was sufficient to detect between-group differences with probability (power) = 0.91. All data were statistically analyzed using SPSS (version 27.0; IBM, Armonk, NY, USA). Descriptive analysis of continuous variables, such as SE or AL, were described as mean ± SD, whereas discrete variables were described as counts (proportions). The Kolmogorov–Smirnov test was used to test the distribution of data. In the parametric analyses between the emmetropia and myopia groups, independent sample *t*-tests were used for normally distributed data and non-parametric tests were used for non-normally distributed data. In the myopia subgroup analyses, the Kruskal–Wallis test was used to assess differences in data between the refractive groups using post hoc tests. For correlation analysis, the Pearson correlation test was used for normally distributed data and the Spearman's correlation test was used for non-normally distributed data. Multiple linear regression models were used to assess relevant factors affecting the longitudinal modulus of the nucleus (LMN) and accommodation. Statistical significance was set at $P < 0.05$.

Results

Participant Characteristics

This study included 195 right eyes from 195 participants (102 male subjects). The cohort consisted of 41 eyes with low myopia, 59 with moderate myopia, and 58 with high myopia; and 37 emmetropic eyes served as controls. Table 1 shows the basic patient demographics. No significant differences were found in age, sex, or IOP among the four groups ($P = 0.507$, $P = 0.161$, and $P = 0.423$, respectively).

Crystalline Lens Biomechanical Properties

LMN and the longitudinal modulus of the anterior cortex (LMAC) and posterior cortex (LMPC) were 3.342 ± 0.023 GPa, 3.015 ± 0.048 GPa, and 2.978 ± 0.049 GPa in emmetropia, and 3.395 ± 0.027 GPa, 3.030 ± 0.066 GPa, and 2.990 ± 0.066 GPa, respectively, in myopia (see Table 1). LMN was significantly higher in myopia than in emmetropia ($P < 0.001$; see Table 1); and LMAC and LMPC showed no difference between the two groups. Within the myopia subgroups, the mean LMN was 3.369 ± 0.030 GPa,

Table 1. Subject Characteristics in Each Refractive Group

Variables	Emmetropia ($n = 37$)	Myopia				*P* Value*	*P* Value†
		Total ($n = 158$)	Low Myopia ($n = 41$)	Moderate Myopia ($n = 59$)	High Myopia ($n = 58$)		
Age, y	22.4 ± 1.8	22.5 ± 4.2	22.4 ± 3.7	23.3 ± 5.0	21.8 ± 3.4	0.696	0.507
Gender, male, *N* (%)	18 (48.6)	84 (53.2)	27 (65.9)	32 (54.2)	25 (43.1)	0.717‡	0.161‡
Intra-ocular pressure, mm Hg	15.8 ± 2.0	16.3 ± 2.2	16.3 ± 2.0	16.5 ± 2.4	16.0 ± 2.2	0.213	0.423
Spherical equivalent, D	−0.13 ± 0.35	−5.06 ± 1.92	−2.58 ± 0.35	−4.50 ± 0.74	−7.15 ± 0.80	**<0.001**	**<0.05**§,‖,¶,**,††,‡‡
Axial length, mm	23.57 ± 0.57	25.88 ± 0.97	24.94 ± 0.67	25.66 ± 0.81	26.69 ± 0.57	**<0.001**	**<0.05**§,‖,¶,**,††,‡‡
Optical coherence tomography (OCT)							
Radius of the anterior lens surface curvature, mm	12.83 ± 1.15	12.32 ± 1.24	12.98 ± 1.06	12.54 ± 1.30	11.69 ± 0.96	**0.023**	**<0.05**§,‖,¶
Radius of the posterior lens surface curvature, mm	6.14 ± 0.33	6.05 ± 0.37	6.16 ± 0.35	6.13 ± 0.35	5.90 ± 0.36	0.186	**<0.05**§,‖,¶
Lens thickness, mm	3.65 ± 0.21	3.60 ± 0.21	3.61 ± 0.21	3.57 ± 0.21	3.63 ± 0.21	0.179	0.288
Lens diameter, mm	9.71 ± 0.42	9.75 ± 0.29	9.71 ± 0.38	9.75 ± 0.23	9.77 ± 0.27	0.883	0.883
Lens densitometry, centerline	44.38 ± 5.41	40.58 ± 6.46	44.17 ± 6.06	42.64 ± 5.37	36.26 ± 5.33	**0.004**	**<0.05**§,‖,¶,**,††
Lens densitometry, pupil (4.0 mm)	37.41 ± 2.65	35.92 ± 4.00	37.80 ± 3.64	36.90 ± 3.57	33.74 ± 3.70	**0.011**	**<0.05**§,‖,¶
Brillouin Optical Microscope							
Longitudinal modulus of nucleus, GPa	3.342 ± 0.023	3.395 ± 0.027	3.369 ± 0.030	3.394 ± 0.023	3.412 ± 0.013	**<0.001**	**<0.05**§,‖,¶,**,††,‡‡
Longitudinal modulus of anterior cortex, GPa	3.015 ± 0.048	3.030 ± 0.066	3.023 ± 0.078	3.023 ± 0.067	3.040 ± 0.056	0.540	0.455
Longitudinal modulus of posterior cortex, GPa	2.978 ± 0.049	2.990 ± 0.066	2.9887 ± 0.075	2.982 ± 0.064	3.001 ± 0.060	0.687	0.402
Width of top plateau, mm	2.606 ± 0.181	2.695 ± 0.228	2.600 ± 0.194	2.648 ± 0.222	2.780 ± 0.253	**0.019**	**<0.05**§,‖,¶
Width of bottom plateau, mm	3.975 ± 0.262	4.077 ± 0.318	4.066 ± 0.401	4.052 ± 0.315	4.109 ± 0.61	0.061	0.090
Accommodation							
Amplitude of accommodation	8.03 ± 1.46	9.34 ± 2.76	7.96 ± 1.16	9.36 ± 2.63	10.86 ± 2.01	**0.002**	**<0.05**§,‖,¶,**,††
Accommodative facility	13.88 ± 4.64	8.04 ± 3.49	11.22 ± 2.43	8.03 ± 3.63	6.15 ± 2.36	**<0.001**	**<0.05**§,‖,¶,**,††,‡‡

The *P* values in bold represent statistically significant differences.
* Statistically significant difference between the total myopia and emmetropia groups.
† Calculated by Kruskal-Wallis test.
‡ Calculated by chi-square test.
§ Statistically significant difference between the high myopia and emmetropia groups.
‖ Statistically significant difference between the high myopia and low myopia groups.
¶ Statistically significant difference between the high myopia and moderate myopia groups.
** Statistically significant difference between the moderate myopia and emmetropia groups.
†† Statistically significant difference between the moderate myopia and low myopia groups.
‡‡ Statistically significant difference between the low myopia and emmetropia groups.

Investigative Ophthalmology & Visual Science

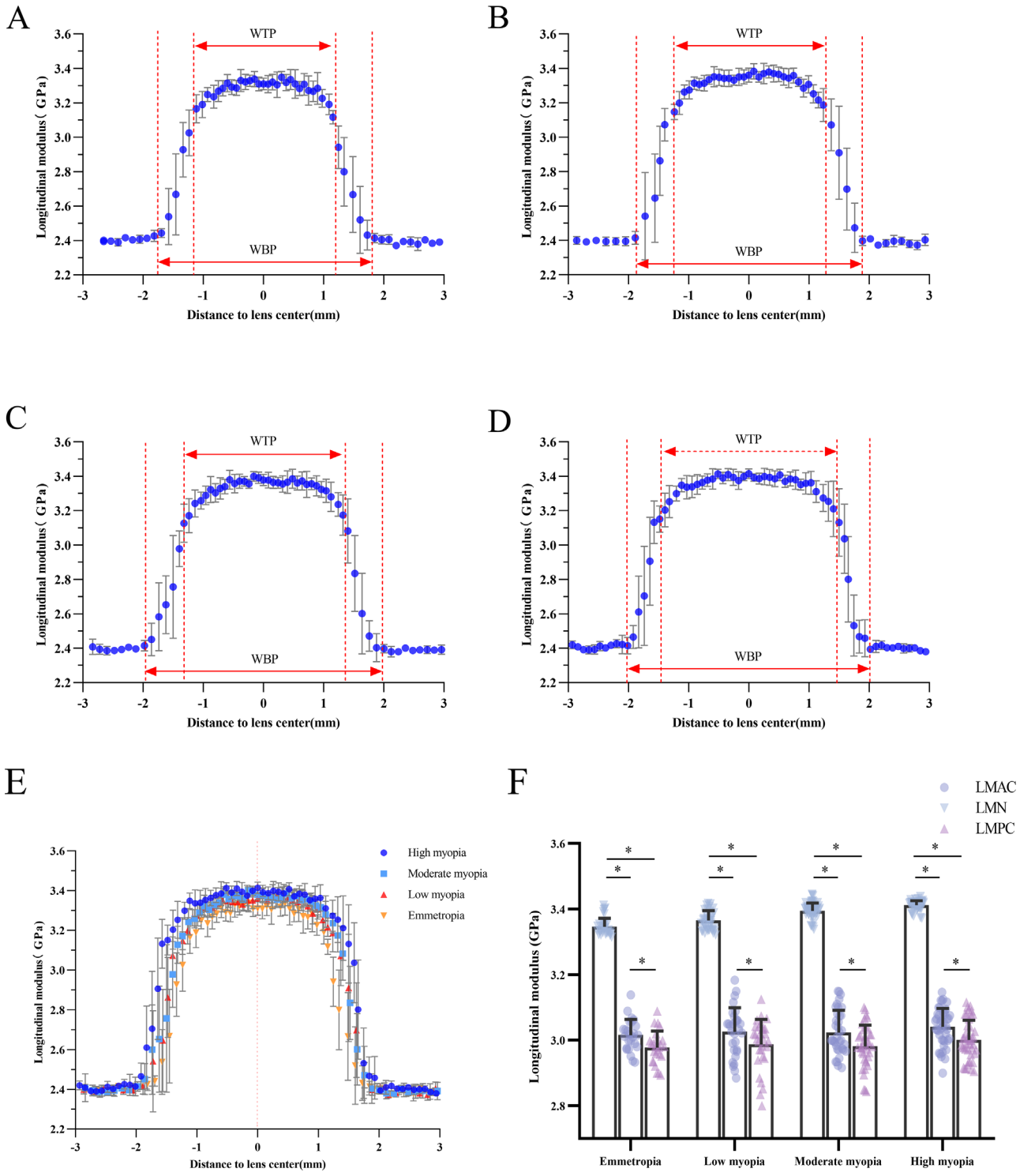

Figure 2. Representative axial profiles of Brillouin optical scans of the lens at different refractive states. (A, **B**, **C**, and **D)** Show representative axial profiles of the Brillouin optical scans of the lens in emmetropia, low myopia, moderate myopia, and high myopia states, respectively. The points and error bars represent the mean and SD. **(E)** Shows a summary of the four groups of lens axial profiles. **(F)** Shows bar charts comparing LMN, LMAC, and LMPC within each refractive group. *$P < 0.05$; LMAC, longitudinal modulus of anterior cortex; LMN, Longitudinal modulus of nucleus; LMPC, longitudinal modulus of posterior cortex; WBP, width of bottom plateau; WTP, width of top plateau.

3.394 ± 0.023 GPa, and 3.412 ± 0.013 GPa in low myopia, moderate myopia, and high myopia groups, respectively, showing significant differences among all groups (all $P < 0.001$; see Table 1). Across all refractive groups, LMN was significantly greater than LMAC and LMPC, whereas LMAC was greater than LMPC (all $P < 0.05$; Fig. 2). Figure 2 shows representative axial profiles of the lens for Brillouin optical scans of different refractive groups.

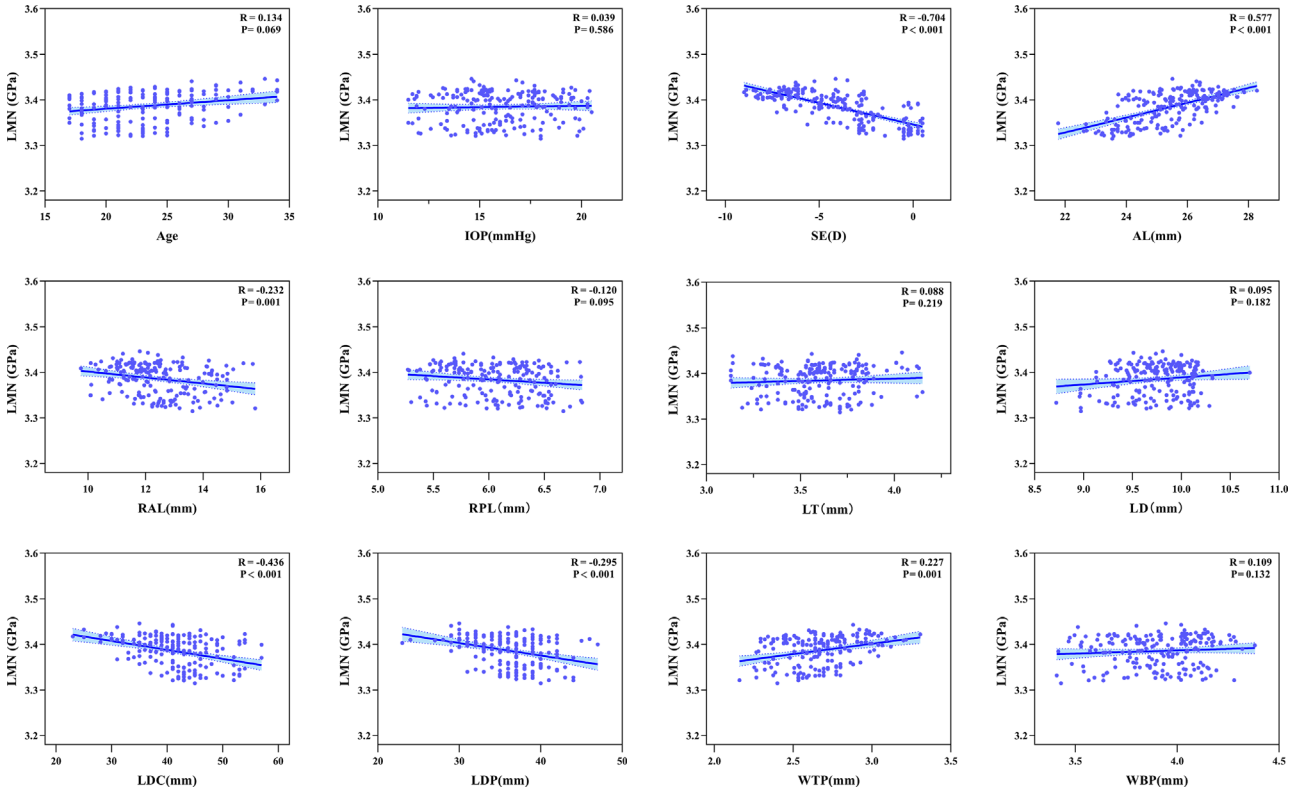

Figure 3. Correlations analysis of LMN with other factors. AL, axial length; LD, lens diameter; LDC, lens densitometry centerline; LDP, lens densitometry pupil (4.0 mm); LMN, longitudinal modulus of nucleus; LT, lens thickness; RAL, radius of the anterior lens surface curvature; RPL, radius of the posterior lens surface curvature; SE, spherical equivalent; WBP, width of bottom plateau; WTP, width of top plateau.

Table 2. Multiple Regression Analysis of Longitudinal Modulus of Lens Nucleus

	Univariate Regression				Multiple Regression (R^2 = 0.605)			
Variables	β	**95% CI**	**Standardized-β**	***P* Value***	β	**95% CI**	**Standardized-β**	***P* Value****
Age, y	0.001	0.000 to 0.002	0.134	0.069	0.002	0.001 to 0.003	0.228	**<0.001**
Gender	0.008	−0.001 to 0.018	0.120	0.094	0.005	−0.002 to 0.011	0.070	0.174
Intra-ocular pressure, mm Hg	0.001	−0.002 to 0.003	0.039	0.586	–			
Spherical equivalent, D	−0.009	−0.011 to −0.008	−0.726	**<0.001**	−0.009	−0.012 to −0.006	−0.712	**<0.001**
Axial length, mm	0.016	0.013 to 0.019	0.606	**<0.001**	0.001	−0.005 to 0.006	0.019	0.859
Radius of the anterior lens surface curvature, mm	−0.006	−0.009 to −0.002	−0.203	**0.001**	0.002	−0.001 to 0.005	0.093	0.093
Radius of the posterior lens surface curvature, mm	−0.011	−0.024 to −0.002	−0.122	0.095	0.003	−0.009 to 0.010	0.03	0.575
Lens thickness, mm	0.003	−0.020 to 0.026	0.019	0.219	–			
Lens diameter, mm	0.010	−0.005 to 0.026	0.097	0.182	–			
Lens densitometry, centerline	−0.002	−0.003 to −0.001	−0.417	**<0.001**	−0.001	−0.002 to 0.000	−0.230	**0.012**
Lens densitometry, pupil (4.0 mm)	−0.002	−0.004 to −0.001	−0.272	**<0.001**	0.001	−0.001 to 0.002	0.074	0.410
Width of top plateau, mm	0.040	0.019 to 0.061	0.268	**0.001**	0.001	−0.015 to 0.018	0.010	0.863
Width of bottom plateau, mm	0.017	−0.005 to 0.039	0.110	0.132	–			

The *P* values in bold represent statistically significant differences.
* Statistical significance was tested by univariate linear regression.
** Statistical significance was tested by multiple linear regression.

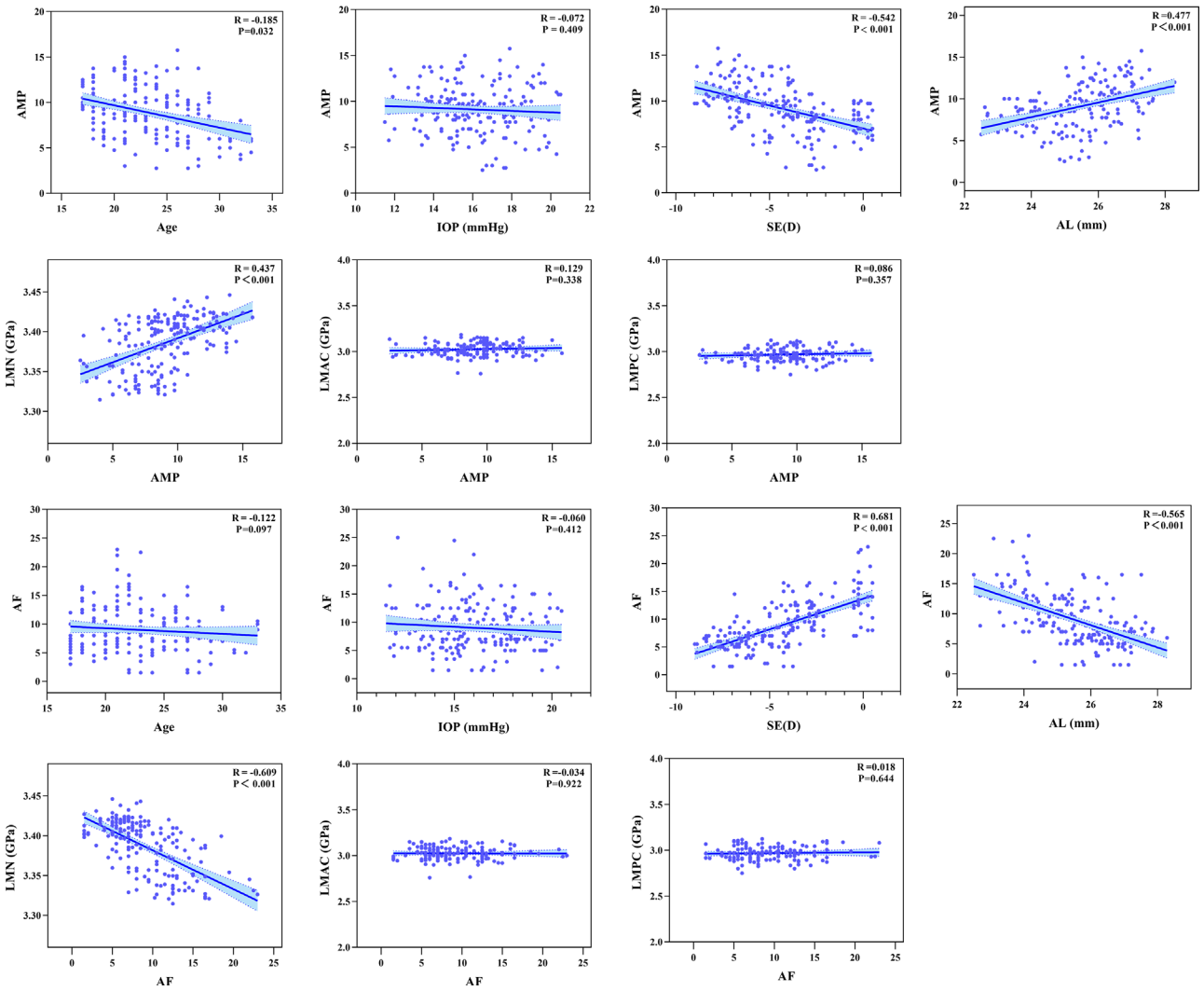

Figure 4. Correlations between AMP, AF, and other factors. AF, accommodative facility; AL, axial length; AMP, amplitude of accommodation; IOP, intraocular pressure; LMN, longitudinal modulus of nucleus; LMAC, longitudinal modulus of anterior cortex; LMPC, longitudinal modulus of posterior cortex; SE, spherical equivalent.

Crystalline Lens Morphology and Accommodation

In lens morphometric analyses, myopic eyes exhibited a greater width of the top plateau (WTP), smaller radius of the anterior lens surface curvature (RAL), and lower lens densitometry in the centerline (LDC) and lens densitometry pupillary (LDP) regions of the lens than emmetropic eyes (all $P < 0.05$; see Table 1). In the subgroup analyses, WTP, RAL, the radius of the posterior lens (RPL) surface curvature, and LDP showed statistically significant differences from the other groups only in the high myopia group (all $P < 0.05$; see Table 1), whereas LDC showed significant differences among the low, moderate, and high myopia groups (all $P < 0.05$; see Table 1). In the accommodation analyses, myopic eyes showed a greater AMP and poorer AF than emmetropic eyes (all $P < 0.05$; see Table 1). In the subgroup analyses, AMP showed significant differences among the groups (all $P < 0.05$; see Table 1), except for emmetropic eyes and low myopic eyes ($P = 0.059$). Significant differences were found among the groups for emmetropia, low myopia, moderate myopia, and high myopia on AF (all $P < 0.05$; see Table 1).

Correlation Analysis Between Crystalline Lens Biomechanical Properties and Crystalline Lens Morphology Parameters

Figure 3 shows scatter plots of LMN versus associated factors. LMN was significantly negatively correlated with SE ($R = -0.704$, $P < 0.001$), significantly positively correlated with AL ($R = 0.577$, $P < 0.001$), and weakly correlated with age ($R = 0.134$, $P = 0.069$). Among the lens morphology parameters, LMN was significantly negatively correlated with RAL, LDC, and LDP ($R = -0.232$, $P = 0.001$; $R = -0.436$, $P < 0.001$; and $R = -0.295$, $P < 0.001$, respectively) and significantly positively correlated with WTP ($R = -0.203$, $P = 0.018$). No significant correlations were found between LMN and sex, IOP, RPL, LT, LD, or width of the bottom plateau. Supplementary Table S1 shows that LMAC had no significant correlation with any other parameter except for LDC ($R = 0.227$, $P = 0.001$). No significant correlation was found between LMPC and any of the parameters (see Supplementary Table S1).

Investigative Ophthalmology & Visual Science

Table 3. Multiple Regression Analysis of Accommodation

	Amplitude of Accommodation						Accommodative Facility					
	Univariate Model			Multivariate Model ($R^2 = 0.278$)			Univariate Model			Multivariate Model ($R^2 = 0.496$)		
Variables	β (95% CI)	Standardized β	*P* Value*	β (95% CI)	Standardized β	*P* Value**	β (95% CI)	Standardized β	*P* Value*	β (95% CI)	Standardized β	*P* Value**
Age, y	−0.106 (−0.202 to −0.009)	−0.158	**0.032**	−0.112 (−0.201 to −0.023)	−0.167	**0.014**	−0.134 (−0.293 to 0.025)	−0.122	0.097	−0.160 (−0.283 to −0.038)	−0.146	**0.010**
Gender	0.584 (−0.176 to 1.343)	0.111	0.131	0.540 (−0.159 to 1.239)	0.103	0.129	−0.234 (−1.486 to 1.019)	−0.027	0.713	0.518 (−0.439 to 1.476)	0.060	0.287
IOP, mm Hg	−0.071 (−0.240 to 0.098)	−0.061	0.409	–			−0.115 (−0.393 to 0.162)	−0.060	0.412	–		
SE, D	−0.500 (−0.631 to −0.369)	−0.486	**0.001**	−0.290 (−0.588 to 0.007)	−0.282	0.056	1.113 (0.928 to 1.297)	0.660	**<0.001**	0.928 (0.521 to 1.336)	0.551	**<0.001**
AL, mm	0.871 (0.579 to 1.144)	0.420	**<0.001**	0.095 (−0.436 to 0.626)	0.046	0.726	−1.868 (−2.281 to −1.455)	−0.550	**<0.001**	0.181 (−0.546 to 0.908)	0.053	0.624
LMN, GPa	33.291 (22.893 to 43.688)	0.422	**<0.001**	15.606 (0.497 to 30.716)	0.198	**0.043**	−79.618 (−94.435 to −64.802)	−0.616	**<0.001**	−30.620 (−51.313 to −9.928)	−0.237	**0.004**
LMAC, GPa	2.905 (−3.067 to 8.877)	0.083	0.338	–			−0.504 (−10.690 to 9.683)	−0.008	0.922	–		
LMPC, GPa	2.735 (−3.115 to 8.584)	0.080	0.357	–			2.335 (−7.633 to 12.303)	0.040	0.644	–		

The *P* values in bold represent statistically significant differences.

AL, axial length; IOP, intraocular pressure; LMAC, longitudinal modulus of anterior cortex; LMN, longitudinal modulus of nucleus; LMPC, longitudinal modulus of posterior cortex; SE, spherical equivalent.

* Statistical significance was tested by univariate linear regression.

** Statistical significance was tested by multiple linear regression.

Multiple Regression Analysis of Longitudinal Modulus of the Nucleus

Table 2 shows a high correlation of LMN with SE ($\beta = -0.009$, 95% confidence interval [CI] = −0.011 to −0.008, $P < 0.001$), AL ($\beta = 0.016$, 95% CI = 0.013 to 0.019, $P < 0.001$), RAL ($\beta = -0.006$, 95% CI = −0.009 to −0.002, $P = 0.001$), LDC ($\beta = -0.002$, 95% CI = −0.003 to −0.001, $P < 0.001$), LDP ($\beta = -0.002$, 95% CI = −0.004 to −0.001, $P < 0.001$), and WTP ($\beta = 0.040$, 95% CI = 0.019 to 0.061, $P = 0.001$) according to one-way linear regression. After adjusting for age and sex, LMN was independently associated with age ($\beta = 0.002$, 95% CI = 0.001 to 0.003, $P < 0.001$), SE ($\beta = -0.009$, 95% CI = −0.012 to −0.006, $P < 0.001$), and LDC ($\beta = -0.001$, 95% CI = −0.002 to 0.000, $P = 0.012$) only in the final multiple regression model (see Table 2).

Correlation Analysis Between Crystalline Lens Biomechanical Properties and Accommodation

Figure 4 shows that AMP was significantly negatively correlated with age and SE ($R = -0.185$, $P = 0.032$; and $R = -0.542$, $P < 0.001$) and significantly positively correlated with AL and LMN ($R = 0.477$, $P < 0.001$; and $R = 0.437$, $P < 0.001$). No significant correlations were observed between the AMP and sex, IOP, LMAC, or LMPC. Correlation analysis showed that AF was significantly positively correlated with SE ($R = 0.681$, $P < 0.001$) and significantly negatively correlated with AL and LMN ($R = -0.565$, $P < 0.001$; and $R = -0.609$, $P < 0.001$). No significant correlations were observed between AF and age, sex, IOP, LMAC, or LMPC.

Multiple Regression Analysis of Accommodation

Table 3 shows high correlation of AMP with age ($\beta = -0.106$, 95% CI = −0.202 to −0.009, $P = 0.032$), SE ($\beta = -0.500$, 95% CI = −0.631 to −0.369, $P < 0.001$), AL ($\beta = 0.871$, 95% CI = 0.579 to 1.144, $P < 0.001$), and LMN ($\beta = 33.291$, 95% CI = 22.893 to 43.688, $P < 0.001$) according to one-way linear regression. After adjusting for age and sex, AMP was independently correlated only with age ($\beta = -0.112$, 95% CI = −0.201 to −0.023, $P = 0.014$) and LMN ($\beta = 15.606$, 95% CI = 0.497 to 30.716, $P = 0.043$) in the final multiple regression model (see Table 3).

One-way linear regression showed a high correlation of AF with SE ($\beta = 1.113$, 95% CI = 0.928 to 1.297, $P < 0.001$), AL ($\beta = -1.868$, 95% CI = −2.281 to −1.455, $P < 0.001$), and LMN ($\beta = -79.618$, 95% CI = −94.435 to −64.802, $P < 0.001$). After adjusting for age and sex, AF was independently correlated only with age ($\beta = -0.160$, 95% CI = −0.283 to −0.038, $P = 0.010$), SE ($\beta = 0.928$, 95% CI = 0.521 to 1.336, $P < 0.001$), and LMN ($\beta = -30.620$, 95% CI = −51.313 to −9.928, $P = 0.004$) in the final multiple regression model (see Table 3).

Discussion

This study presented an in vivo analysis of biomechanical properties of the lens and their potential influences on adult emmetropic and myopic eyes. Furthermore, it explored for the first time the association between lens biomechanical properties and accommodation. The findings showed that the mean LMN, LMAC, and LMPC were 3.342 ± 0.023

GPa, 3.015 ± 0.048 GPa, and 2.978 ± 0.049 GPa, respectively, in emmetropia and 3.395 ± 0.027 GPa, 3.030 ± 0.066 GPa, and 2.990 ± 0.066 GPa, respectively, in myopia. The LMN of myopic eyes was significantly higher than that of emmetropic eyes and it tended to increase significantly as the degree of myopia increased. Further analysis revealed that LDC was independently negatively correlated with LMN, an association that may involve changes in lens microstructure. In terms of accommodation, our study found that a larger LMN was strongly associated with a larger AMP and poorer AF. These findings provide a new perspective for a deeper understanding of the pathogenesis of myopia.

The crystalline lens, an important refractive medium in the eye, plays a key role in the pathophysiology of myopia.[31,32] However, previous studies have focused on changes in myopic lens morphology, and there is a relative paucity of research on lens biomechanics.[8,33–35] Our study took a biomechanical perspective and found that myopic eyes had a larger LMN than emmetropic eyes and that LMN was increased significantly with increasing myopia. Although LMN is not directly equivalent to elastic modulus or shear modulus, LMN provides information about the intrinsic stiffness of a material at the microscopic level. Moreover, it has been shown that the Brillouin longitudinal modulus correlates with the Young's modulus in soft biological tissues.[26] Higher LMN indicates an increase in the stiffness and a decrease in the compressibility of the lens nucleus, which may indirectly indicate a decrease in the deformability of the lens nucleus in response to physiological forces (e.g. accommodative forces), which may affect accommodation and exacerbate the development of myopia.[9,10,36] To understand the mechanisms underlying this phenomenon, we examined the potential factors affecting LMN and found that LDC was the only lens parameter that was significantly negatively correlated with LMN in the LMN multiple regression model. This suggests that the biomechanical properties of the lens are closely related to its internal structural arrangement. Lens transparency and viscoelasticity have been found to be positively correlated with the lens protein concentration.[37–40] The increase in LMN in myopic eyes may be related to the upregulation of lens protein expression in myopic eyes.[41] However, the relationship between specific protein components and the optical and biomechanical properties of the lens needs to be determined in further studies.

The LMN reported in our study for young emmetropic eyes (3.342 ± 0.023 GPa) was higher than the range of 2.81 to 3.11 GPa reported by Besner et al.[18] This difference may be attributed to variations in sample characteristics, including age, gender, and racial differences, etc. Future studies need to focus on differences in lens biomechanical properties across sample characteristics. Additionally, our study found that the distribution of stiffness within the lens was heterogeneous; that is, the lens nucleus was harder than its cortex, and the anterior cortex was harder than the posterior cortex in all refractive groups. These differences in the lens' internal hardness distribution suggested that the lens material properties could not be modeled as a simple or isomorphic structural entity in future studies, especially in those using approaches such as finite element modeling of the lens.[42,43] During accommodation, the tension of the suspensory ligament must be transmitted to the lens nucleus via the lens cortex to deform and change the refractive power.[9] The differences in cortical stiffness between the anterior and posterior cortices indicated that the distribution of the accommodation force on the lens nucleus was non-uniform, which provided new clues for understanding the physiological mechanism of accommodation.

By further analyzing the association between lens biomechanical properties and accommodation, our study found that greater LMN was significantly correlated with greater AMP and poorer AF, suggesting that lens nuclear biomechanical properties played a key role in the lens response to accommodation stimulus.[9] This study measured AMP using the minus lens method, which primarily reflects the eye's ability to maximize accommodation under monocular conditions. The AMP measured by this method is influenced by the combined biomechanical properties of the forces exerted by the lens capsule, lens nucleus, and ciliary muscles.[44] Our study found that LMN was the only ocular parameter positively correlated with AMP in the AMP multiple regression model, a finding that may reflect a unique compensatory mechanism of accommodation in young patients with myopia: stronger ciliary muscle contractility and capsular elasticity may be able to synergistically overcome lens stiffening in order to maintain a higher AMP.[44,45] Future studies should add assessment of ciliary muscle function to provide a more comprehensive understanding of the mechanisms by which multiple tissues synergistically regulate AMP. Additionally, subjective AMP is affected by the eye's depth of focus. High retinal image blur thresholds in patients with myopia may increase the depth of focus, thus manifesting as an increase in AMP.[46,47]

Accuracy of accommodation has long been associated with the development of refractive errors, with inaccurate accommodation responses preventing the formation of a stable and clear retinal image in the eye.[11,48,49] AF is an important measure of the accuracy and speed of a participant's accommodation response.[50,51] Our study found a significant positive correlation between AF and SE, with a significant decrease in AF in myopic eyes compared with that in emmetropic eyes. Mutti et al.[52] hypothesized that this defect in the accommodation response may be due to increased resistance to accommodation as a result of increased lens tension, a hypothesis that may be indirectly supported by our findings. Our study found a significant negative correlation between AF and LMN, suggesting that a high LMN may resist the tension exerted by the ciliary muscle during accommodation and that a large resistance to accommodation prevents the lens from responding quickly to the accommodation stimulus, reducing AF. Decreased AF further exacerbates the risk of progression of myopia.[49,53] The AF test used in this study measured the combined process of accommodation stimulus and relaxation. Future studies with more specific methodologies are needed to distinguish the effects of LMN on these two phases of accommodation. It is worth noting that AF, measured over time, may be related to the viscoelasticity of the lens, which could be a direction for future research.

Regarding age-related trends, the LMN in our study was increased with age in the range of 18 to 34 years, similar to the findings of previous studies on age-related lens sclerosis,[13,16,36,54] which may be related to growing, compressed lens fibers.[55] Conversely, the longitudinal modulus of the lens cortex did not show a correlation with age. Another interesting finding of this study was that lens nucleus thickness was significantly increased in highly myopic eyes, but the total lens thickness did not differ between the groups, suggesting that the lens nucleus is more closely associated with high myopia relative to the lens cortex. It should be noted, however, that whether the increased thickness of the

Investigative Ophthalmology & Visual Science

lens nucleus is a cause or a consequence of myopia is still unclear and requires further study.

Our study has some limitations. First, it included only Chinese participants, with a relatively small sample size and relatively young age. Future studies with larger sample sizes and greater ethnic diversity are needed to validate our findings. Second, Brillouin lens testing in our study could not be performed with the participants' refractive status corrected; therefore, inevitably, there would be interference from accommodation factors. Third, as a cross-sectional study, the current findings do not allow for the confirmation of a causal relationship among lens biomechanical properties, lens structure, and accommodation, and follow-up studies with longitudinal results are needed. Finally, the mechanical moduli reported by Brillouin scattering and classical methods are not directly comparable and reflect different aspects of tissue mechanics. Future studies should aim to integrate these complementary approaches to provide a more comprehensive understanding of tissue mechanics across different scales.

Conclusions

This study investigated, for the first time, the in vivo biomechanical distribution characteristics of the lens in adult emmetropic and myopic eyes using the BOSS. LMN was significantly negatively correlated with SE. An increase in LMN in myopic eyes was significantly associated with a decrease in AF and an increase in AMP. High LMN may be an important biological alteration during the development of myopia, especially high myopia, and help further investigate the pathogenesis of myopia.

Acknowledgments

The authors thank all the participants who made this study possible, and Editage (https://www.editage.cn) for English language editing.

Supported by the National Natural Science Foundation of China (Grant No. 82271118), Tianjin Health Research Project (No. TJWJ2022XK036), Tianjin Key Medical Discipline (Specialty) Construction Project (no. TJYXZDXK-016A), and Tianjin Natural Science Foundation (21JCQNJC01000).

Credit Authorship Contribution Statements: Le Chang: Conceptualization, Data curation, Formal analysis, Methodology, Writing – original draft, Writing – review and editing. **Fen Song:** Data curation, Formal analysis, Methodology, Validation, Writing – review and editing. **Shijia Qu:** Methodology, Writing – review and editing, Data curation. **Huazheng Cao:** Data curation, Methodology, Writing – review and editing. **Yanan Wu:** Data curation, Writing – review and editing. **Lulu Xu:** Methodology, Writing – review and editing. **Jing Wang:** Methodology, Writing – review and editing. **Ruirui Zhang:** Methodology, Writing – review and editing. **Chao Xue:** Supervision, Writing – review and editing. **Yan Wang:** Conceptualization, Data curation, Formal analysis, Funding acquisition, Methodology, Supervision, Visualization, Writing – original draft, Writing – review and editing.

Data Availability: The data that support the findings of this study are available from the corresponding author upon reasonable request.

Disclosure: **L. Chang**, None; **F. Song**, None; **S. Qu**, None; **H. Cao**, None; **Y. Wu**, None; **L. Xu**, None; **J. Wang**, None; **R. Zhang**, None; **C. Xue**, None; **Y. Wang**, None

References

1. Holden BA, Fricke TR, Wilson DA, et al. Global prevalence of myopia and high myopia and temporal trends from 2000 through 2050. *Ophthalmology*. 2016;123(5):1036–1042.
2. Pan CW, Ramamurthy D, Saw SM. Worldwide prevalence and risk factors for myopia. *Ophthalmic Physiol Opt*. 2012;32(1):3–16.
3. Wong YL, Saw SM. Epidemiology of pathologic myopia in Asia and worldwide. *Asia Pac J Ophthalmol (Phila)*. 2016;5(6):394–402.
4. Iribarren R. Crystalline lens and refractive development. *Prog Retin Eye Res*. 2015;47:86–106.
5. Zhang Y, Zhang J, Jin A, et al. Interocular difference in crystalline lens morphology in children and adolescents with unilateral high myopia. *Asia Pac J Ophthalmol (Phila)*. 2024;13(1):100001.
6. Mutti DO, Mitchell GL, Sinnott LT, et al. Corneal and crystalline lens dimensions before and after myopia onset. *Optom Vis Sci*. 2012;89(3):251–262.
7. Shen L, Wei C, Yang W, et al. Analysis of the relationship between lens morphology and aberrations in patients with myopia: a cross-sectional study. *Int Ophthalmol*. 2023;43(12):4911–4919.
8. Bolz M, Prinz A, Drexler W, Findl O. Linear relationship of refractive and biometric lenticular changes during accommodation in emmetropic and myopic eyes. *Br J Ophthalmol*. 2007;91(3):360–365.
9. Wang K, Pierscionek BK. Biomechanics of the human lens and accommodative system: functional relevance to physiological states. *Prog Retin Eye Res*. 2019;71:114–131.
10. de la Hoz A, Martinez-Enriquez E, Marcos S. Estimation of crystalline lens material properties from patient accommodation data and finite element models. *Invest Ophthalmol Vis Sci*. 2023;64(11):31.
11. Logan NS, Radhakrishnan H, Cruickshank FE, et al. IMI Accommodation and binocular vision in myopia development and progression. *Invest Ophthalmol Vis Sci*. 2021;62(5):4.
12. Cheng T, Deng J, Xiong S, et al. Crystalline lens power and associated factors in highly myopic children and adolescents aged 4 to 19 years. *Am J Ophthalmol*. 2021;223:169–177.
13. Wilde GS, Burd HJ, Judge SJ. Shear modulus data for the human lens determined from a spinning lens test. *Exp Eye Res*. 2012;97(1):36–48.
14. Burd HJ, Wilde GS, Judge SJ. An improved spinning lens test to determine the stiffness of the human lens. *Exp Eye Res*. 2011;92(1):28–39.
15. Weeber HA, Eckert G, Soergel F, Meyer CH, Pechhold W, van der Heijde RG. Dynamic mechanical properties of human lenses. *Exp Eye Res*. 2005;80(3):425–434.
16. Weeber HA, Eckert G, Pechhold W, van der Heijde RG. Stiffness gradient in the crystalline lens. *Graefes Arch Clin Exp Ophthalmol*. 2007;245(9):1357–1366.
17. Hollman KW, O'Donnell M, Erpelding TN. Mapping elasticity in human lenses using bubble-based acoustic radiation force. *Exp Eye Res*. 2007;85(6):890–893.
18. Besner S, Scarcelli G, Pineda R, Yun SH. In vivo Brillouin analysis of the aging crystalline lens. *Invest Ophthalmol Vis Sci*. 2016;57(13):5093–5100.
19. Manns F, Parel JM, Denham D, et al. Optomechanical response of human and monkey lenses in a lens stretcher. *Invest Ophthalmol Vis Sci*. 2007;48(7):3260–3268.
20. Schachar RA, Chan RW, Fu M. Viscoelastic properties of fresh human lenses under 40 years of age: implications for the aetiology of presbyopia. *Br J Ophthalmol*. 2011;95(7):1010–1013.

21. Hannah G, Andrew S, Claire SB, et al. Repeatability and reproducibility of anterior segment stiffness measurements with a novel Brillouin scanning device. *Invest Ophthalmol Vis Sci*. 2023;64(8):3439.
22. Vaughan JM, Randall JT. Brillouin scattering, density and elastic properties of the lens and cornea of the eye. *Nature*. 1980;284(5755):489–491.
23. Scarcelli G, Yun SH. Confocal Brillouin microscopy for three-dimensional mechanical imaging. *Nat Photonics*. 2007;2:39–43.
24. Yun SH, Chernyak D. Brillouin microscopy: assessing ocular tissue biomechanics. *Curr Opin Ophthalmol*. 2018;29(4):299–305.
25. Eltony AM, Shao P, Yun SH. Measuring mechanical anisotropy of the cornea with Brillouin microscopy. *Nat Commun*. 2022;13(1):1354.
26. Scarcelli G, Kim P, Yun SH. In vivo measurement of age-related stiffening in the crystalline lens by Brillouin optical microscopy. *Biophys J*. 2011;101(6):1539–1545.
27. Zhang H, Asroui L, Tarib I, et al. Motion-tracking brillouin microscopy evaluation of normal, keratoconic, and post-laser vision correction corneas. *Am J Ophthalmol*. 2023;254:128–140.
28. Flitcroft DI, He M, Jonas JB, et al. IMI - Defining and classifying myopia: a proposed set of standards for clinical and epidemiologic studies. *Invest Ophthalmol Vis Sci*. 2019;60(3):M20–M30.
29. Hainsworth DP, Gao X, Bebu I, et al. Refractive error and retinopathy outcomes in type 1 diabetes: the diabetes control and complications trial/epidemiology of diabetes interventions and complications study. *Ophthalmology*. 2021;128(4):554–560.
30. Sliney DH, Aron-Rosa D, DeLori F, et al. Adjustment of guidelines for exposure of the eye to optical radiation from ocular instruments: statement from a task group of the International Commission on Non-Ionizing Radiation Protection (ICNIRP). *Appl Opt*. 2005;44(11):2162.
31. Zhang G, Wei Q, Lu L, Lin AL, Qu C. The evolution of mechanism of accommodation and a novel hypothesis. *Graefes Arch Clin Exp Ophthalmol*. 2023;261(11):3083–3095.
32. Pan Y, Liu Z, Zhang H. Research progress of lens zonules. *Adv Ophthalmol Pract Res*. 2023;3(2):80–85.
33. Wang X, Zhu C, Hu X, et al. Changes in dimensions and functions of crystalline lens in high myopia using CASIA2 optical coherence tomography. *Ophthalmic Res*. 2022;65(6):712–721.
34. Han X, Xiong R, Jin L, et al. Longitudinal changes in lens thickness and lens power among persistent non-myopic and myopic children. *Invest Ophthalmol Vis Sci*. 2022;63(10):10.
35. Wang Y, Liu Y, Zhu X, Zhou X, He JC, Qu X. Corneal and lenticular biometry in Chinese children with myopia. *Clin Exp Optom*. 2023;106(8):836–844.
36. Heys KR, Cram SL, Truscott RJ. Massive increase in the stiffness of the human lens nucleus with age: the basis for presbyopia. *Mol Vis*. 2004;10:956–963.
37. Andley UP. Crystallins in the eye: function and pathology. *Prog Retin Eye Res*. 2007;26(1):78–98.
38. Wang YH, Zhong J, Li XM. Age-related changes of lens thickness and density in different age phases. *Int J Ophthalmol*. 2022;15(10):1591–1597.
39. Bassnett S, Costello MJ. The cause and consequence of fiber cell compaction in the vertebrate lens. *Exp Eye Res*. 2017;156:50–57.
40. Takemoto L, Sorensen CM. Protein-protein interactions and lens transparency. *Exp Eye Res*. 2008;87(6):496–501.
41. Zhu X, Du Y, Li D, et al. Aberrant TGF-β1 signaling activation by MAF underlies pathological lens growth in high myopia. *Nat Commun*. 2021;12(1):2102.
42. Reiss S, Sperlich K, Hovakimyan M, et al. Ex vivo measurement of postmortem tissue changes in the crystalline lens by Brillouin spectroscopy and confocal reflectance microscopy. *IEEE Trans Biomed Eng*. 2012;59(8):2348–2354.
43. Jones CE, Atchison DA, Meder R, Pope JM. Refractive index distribution and optical properties of the isolated human lens measured using magnetic resonance imaging (MRI). *Vision Res*. 2005;45(18):2352–2366.
44. Zhang G, Wei Q, Lu L, Lin AL, Qu C. The evolution of mechanism of accommodation and a novel hypothesis. *Graefes Arch Clin Exp Ophthalmol*. 2023;261(11):3083–3095.
45. Avetisov KS, Bakhchieva NA, Avetisov SE, et al. Biomechanical properties of the lens capsule: a review. *J Mech Behav Biomed Mater*. 2020;101:103446.
46. Day M, Seidel D, Gray LS, Strang NC. The effect of modulating ocular depth of focus upon accommodation microfluctuations in myopic and emmetropic subjects. *Vision Res*. 2009;49(2):211–218.
47. McBrien NA, Millodot M. Amplitude of accommodation and refractive error. *Invest Ophthalmol Vis Sci*. 1986;27(7):1187–1190.
48. Mutti DO, Mitchell GL, Hayes JR, et al. Accommodative lag before and after the onset of myopia. *Invest Ophthalmol Vis Sci*. 2006;47(3):837–846.
49. Chen AH, Ahmad A, Kearney S, Strang N. The influence of age, refractive error, visual demand and lighting conditions on accommodative ability in Malay children and adults. *Graefes Arch Clin Exp Ophthalmol*. 2019;257(9):1997–2004.
50. Meng C, Zhang Y, Wang S. Changes in accommodation and convergence function after refractive surgery in myopic patients. *Eur J Ophthalmol*. 2023;33(1):29–34.
51. Prousali E, Haidich AB, Tzamalis A, Ziakas N, Mataftsi A. The role of accommodative function in myopic development: a review.. *Semin Ophthalmol*. 2022;37(4):455–461.
52. Mutti DO, Jones LA, Moeschberger ML, Zadnik K. AC/A ratio, age, and refractive error in children. *Invest Ophthalmol Vis Sci*. 2000;41(9):2469–2478.
53. Allen PM, O'Leary DJ. Accommodation functions: co-dependency and relationship to refractive error. *Vision Res*. 2006;46(4):491–505.
54. Zhou H, Yan H, Yan W, Wang X, Li Q. In vivo ultraosound elastographic evaluation of the age-related change of human lens nuclear stiffness. *BMC Ophthalmol*. 2020;20(1):135.
55. Donaldson PJ, Grey AC, Maceo Heilman B, Lim JC, Vaghefi E. The physiological optics of the lens. *Prog Retin Eye Res*. 2017;56:e1–e24.

Investigative Ophthalmology & Visual Science